calculations show that the swelling substantially influences the infiltration into the clay soil.

LITERATURE CITED

1. A. A. Rode, Soil Water [in Russian], Izd. Akad. Nauk SSSR, Moscow (1952).
2. M. Kutilek, Vodohospodarška Pedologie, SNTL/ALFA, Prague (1978).
3. P. S. Panin, Salt Release in Washed Soils [in Russian], Nauka, Novosibirsk (1968).
4. H. Frenkel and J. D. Rhoades, "Effects of dispersion and swelling on soil hydraulic conductivity," Test. Eval., 6, No. 1 (1978).
5. W. D. Kemper, I. Shainberg, and J. P. Quirk, "Swelling pressures, electric potential and ion concentrations: their role in hydraulic and osmotic flow through clays," Soil Sci. Soc. Amer. Proc., 36, No. 2 (1972).
6. L. S. Leibenzon, The Motion of Natural Liquids and Gases in Porous Media [in Russian], Gostekhizdat, Moscow (1947).
7. Advances in Research on Infiltration Theory in the USSR [in Russian], Nauka, Moscow (1969).
8. V. I. Pen'kovskii and S. T. Rybakova, "Forecasting water-salt conditions in irrigated areas," in: Natural Conditions in Western Siberia and the Transfer of River Flow to Central Asia [in Russian], Nauka, Novosibirsk (1975).

GROWTH AND COLLAPSE OF VAPOR BUBBLES IN BOILING LIQUID

F. B. Nagiev and N. S. Khabeev

UDC 532.529

A study is made of the dynamics and heat-mass exchange of vapor bubbles in water and cryogenic liquids under the action of an abrupt pressure change, which corresponds to bubble behavior in a shock wave, when the wave enters a bubble curtain. Behavior under varying pressure is also studied.

A system of basic equations describing the heat-mass exchange processes and dynamics of a spherical homobaric bubble in a liquid was presented in [1]. The equations of heat adflux, continuity, and state in spherical Euler coordinates (r, t) have the form

$$\begin{gathered}\rho_v\left(\frac{\partial u_v}{\partial t}+v_v\frac{\partial u_v}{\partial r}\right)=\frac{1}{r^2}\frac{\partial}{\partial r}\left(\lambda_v r^2\frac{\partial T_v}{\partial r}\right)+\frac{p_v}{\rho_v}\frac{d\rho_v}{dt},\\ \frac{\partial\rho_v}{\partial t}+\frac{1}{r^2}\frac{\partial}{\partial r}(r^2\rho_v v_v)=0,\quad p_v(t)=B\rho_v(r,t)\,T_v(r,t),\\ \rho_l\left(\frac{\partial u_l}{\partial t}+v_l\frac{\partial u_l}{\partial r}\right)=\frac{1}{r^2}\frac{\partial}{\partial r}\left(\lambda_l r^2\frac{\partial T_l}{\partial r}\right),\\ v_l=w_l R^2/r^2,\quad u_l=c_l T_l,\quad u_v=c_V T_v,\quad \rho_l=\text{const},\end{gathered}\tag{1}$$

where ρ is the density; T, temperature; p, pressure; v, velocity; u, specific internal energy; λ, thermal conductivity coefficient; R, bubble radius; w_l, mass velocity of liquid on bubble surface; B, gas constant; c_V, specific heat of vapor at constant volume. The subscripts l and v refer to liquid and vapor parameters, respectively, while the subscript 0 indicates parameters in the unperturbed state.

The boundary conditions for the heat adflux equations have the form

$$\begin{gathered}r=0,\ \partial T_v/\partial r=0,\\ r=\infty,\ T_l=T_0,\\ r=R(t),\quad \lambda_l\frac{\partial T_l}{\partial r}-\lambda_v\frac{\partial T_v}{\partial r}=jl,\quad T_s=T_l=T_s(p_v),\end{gathered}\tag{2}$$

where $T_S(p_V)$ is the saturation temperature; j is the rate of phase conversion per unit surface; l is the latent heat of evaporation. The last condition defines the so-called quasi-equilibrium approximation. The bubble

Moscow. Translated from Zhurnal Prikladnoi Mekhaniki i Tekhnicheskoi Fiziki, No. 5, pp. 100-106, September-October, 1981. Original article submitted July 24, 1980.

0021-8944/81/2205-0678$07.50

surface velocity and the phase mass velocities on this surface are related by the expressions

$$\dot{R} = w_l + j/\rho_l, \quad \dot{R} = w_v + j/\rho_v(R). \tag{3}$$

The bubble pulsation equation in the presence of phase transitions is written in the form [2]

$$R\dot{w}_l + \frac{3}{2} w_l^2 + \frac{2jw_l}{\rho_l} = \frac{p_v - p_\infty - 2\sigma/R}{\rho_l} - 4\frac{\nu}{R} w_l, \tag{4}$$

where p_∞ is the liquid pressure far from the bubble; σ, surface tension coefficient; ν, kinematic viscosity coefficient.

In fulfilling the homobaric condition, when the bubble size is significantly less than the length of a sound wave in the vapor, the equation of heat adflux in the vapor phase has an integral

$$\frac{dp_v}{dt} = \frac{3(\gamma - 1)}{R}\left(\lambda_v \frac{\partial T_v}{\partial r}\right)_R - \frac{3\gamma p_v}{R} w_v. \tag{5}$$

The homobaric condition also permits definition of the velocity profile within the bubble by integration of the vapor phase continuity equation with consideration of the boundary conditions $v_V(0, t) = 0$, $v_V(R, t) = w_V$:

$$v_v(r, t) = \frac{r}{R} w_v + \frac{\gamma - 1}{\gamma p_v}\left[\lambda_v \frac{\partial T_v}{\partial r}(r, t) - \frac{r}{R}\left(\lambda_v \frac{\partial T_v}{\partial r}\right)_R\right], \tag{6}$$

where γ is the adiabatic index of the vapor.

In [1] the above system of equations was solved numerically for various regimes of radial bubble motion in water under conditions close to normal. In the present study we will examine the dynamics of vapor bubbles in water under high pressure, and also in cryogenic liquids.

Figure 1 shows curves of bubble radius and internal pressure (dashed curves) as functions of time for growth of bubbles with initial radii of $R_0 = 5$, 7, 10 μm (curves 1-3), when the liquid pressure far from the bubble is abruptly reduced from $p_0 = 4 \cdot 10^6$ Pa to $p_l = 2 \cdot 10^6$ Pa. Figure 2 shows the characteristic temperature distribution corresponding to curve 3 of Fig. 1. Curves 1-5 correspond to times t = 0.05, 0.1, 0.3, 0.6, 0.9 μsec. Here $R^* = R/R_0$, $P = p_V/p_0$, $\Theta = T/T_0$, $\xi = r/R$. The initial temperature in the system was homogeneous and equal to the saturation temperature corresponding to equilibrium pressure within the bubble: $T_0 = T_S(p^0)$, $p^0 = p_0 + 2\sigma/R_0$. For greater clarity the spatial scales for vapor and liquid phases are different.

It is evident from Figs. 1 and 2 that with passage of a certain time the pressures within bubble and liquid equalize, the temperature of the vapor within the bubble gradually reduces to the saturation temperature corresponding to the external pressure p_l, and further bubble growth occurs in the thermal regime [3]. The temperature distribution in the liquid enters a self-similar regime, in which the temperature is dependent solely on $\xi = r/R(t)$ [4]. Thus, at high pressures the behavior of gas bubbles with a dropoff in pressure is qualitatively the same as under normal conditions [1]. However, at high parameter values, where the thermophysical properties of vapor and liquid approach each other, the role of internal thermal energy increases.

We note that the temperature of the vapor in the bubble is practically homogeneous and equal to the saturation temperature not only under the usually employed but seldom realizable condition that the bubble size be less than the thickness of the thermodiffusion layer in the vapor $R < (a_V/\omega)^{1/2}$, but also under the condition $c_p T_S/l \approx 1$, where a_V is the thermal diffusivity of the vapor, c_p is the vapor specific heat at constant pressure, and ω is the frequency of radial bubble oscillation. In fact, it follows from the equation for energy in the vapor phase, Eq. (1), that vapor heating in the central part of the bubble where there are no large temperature gradients is defined by the approximate equation

$$\rho_v c_p dT_v/dt \approx dp_v/dt. \tag{7}$$

Using the Clapeyron–Clausius relationships under conditions far from critical, where $\rho_V \ll \rho_l$, one can write

$$\frac{dp_v}{dt} = \frac{l\rho_v}{T_S}\frac{dT_S}{dt}. \tag{8}$$

Substituting Eq. (8) in Eq. (7), we find

$$\frac{c_p T_S}{l}\frac{dT_v}{dt} \approx \frac{dT_S}{dt}. \tag{9}$$

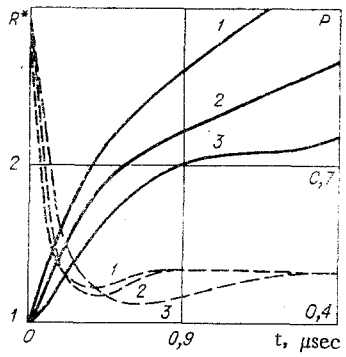

Fig. 1

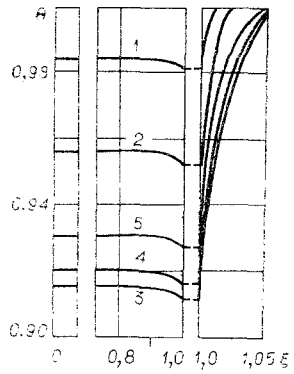

Fig. 2

It is evident from Eq. (9) that at $A = c_V T_S / l \approx 1$ (under atmospheric pressure this occurs, for example, for liquid helium, and also occurs for water at $p \sim 3 \cdot 10^6$ Pa) $T_V \approx T_S$, and the amount of deviation of the parameter A from unity characterizes the deviation of the temperature in the center of a sufficiently large bubble from the surface temperature $T_S(p_V)$.

The bubble heat capacity along the phase equilibrium curve is written in the form [5]

$$c_S = c_p - T\left(\frac{dp}{dT}\right)_S \frac{\partial}{\partial T}\left(\frac{1}{\rho}\right)_p \approx c_p - \frac{l}{T_S}. \tag{10}$$

For the majority of liquids, in particular, for water, under normal conditions $c_S < 0$. This means that for the vapor to remain saturated during compression heat must be removed from it.

If we integrate the equation of heat adflux (1) over the bubble volume (given its homogeneity) we then obtain an expression for the total flux into the vapor phase on the bubble surface

$$\lambda_v \frac{\partial T_v}{\partial r}\Big|_R = \frac{c_S T_S}{l} \frac{R}{3} \frac{dp_v}{dt}. \tag{11}$$

From Eqs. (10), (11) it is evident that at $A = 1$ $c_S = 0$ and the heat flux into the vapor bubble is equal to zero.

From Eqs. (2), (10), (11) it follows that

$$\lambda_l \frac{\partial T_l}{\partial r}\Big|_R = \frac{R\dot{p}_v}{3} \varphi(A, \gamma) + \frac{\gamma p_v \dot{R}}{(\gamma-1)A}, \tag{12}$$

where $\varphi(A, \gamma) = \frac{1}{(\gamma-1)A} + \frac{(A-1)^2}{A}$.

Normally the thermal flux into the vapor phase is neglected in Eq. (2), which corresponds to approximation by the term $(A-1)^2/A$ in $\varphi(A, \gamma)$. From Eq. (12) it is evident that this is admissible if

$$(A-1)^2 \ll 1/(\gamma-1). \tag{13}$$

Equation (13) was obtained assuming homogeneity of bubble parameters, i.e., strictly speaking, for sufficiently small bubbles. At high parameter values where the properties of vapor and liquid approach each other, the unjustified assumption of homogeneity in bubble parameters can lead to significant errors.

Figure 3 shows characteristic temperature distributions for pulsations of vapor bubbles of two different sizes in water, produced by instantaneous increase in liquid pressure far from the bubble from $p_0 = 4 \cdot 10^6$ Pa to $p_l = 8 \cdot 10^6$ Pa (a: $R_0 = 0.01$ mm; b: $R_0 = 1$ mm), with $T_0 = T_S(p^0)$. Curves 1-6 correspond to times $\omega t = 0$, $2\pi/5$, $4\pi/5$, $6\pi/5$, $8\pi/5$, 2π, while $\omega t = 0$ and 2π are two successive times of maximum bubble compression. As is evident from Fig. 3, the temperature distribution curves are nonmonotonic, with temperature "wells" appearing in certain time intervals. In the variant under consideration $c_S > 0$; therefore upon compression the temperature at the bubble center is less than the surface temperature $T_S(p_V)$.

Figure 4 shows a comparison of theoretically calculated radius-time curves with experimental data [6] on bubble growth in liquid nitrogen with gradual pressure decrease from $p_0 = 153 \cdot 10^3$ Pa to $p_l = 116 \cdot 10^3$ Pa corresponding to curve 5. Initial bubble radius $R_0 = 0.4$ mm; initial temperature in the system was homogeneous and corresponded to the saturation temperature $T_0 = T_S(p^0)$. Curve 1 is a solution of the problem in

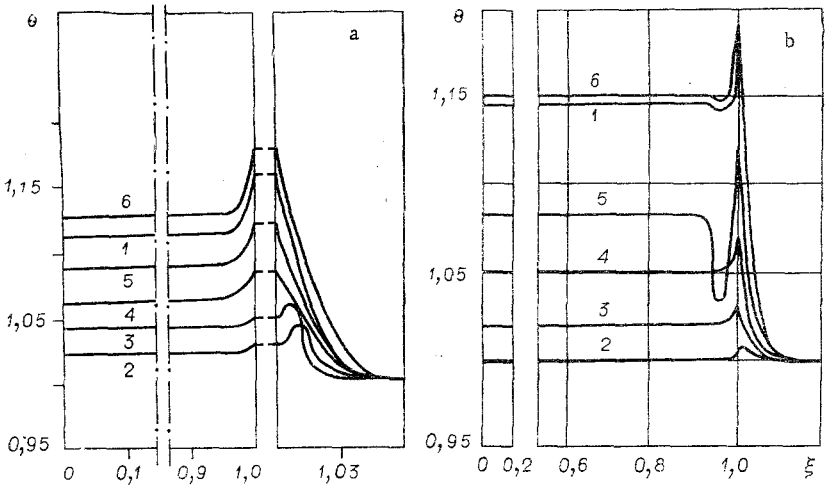

Fig. 3

the full formulation of [1] as presented here; curve 2 is an inertial Rayleigh solution obtained by numerical integration of Eq. (4) with $p_V = 153 \cdot 10^3$ Pa, $p_\infty(t)$ corresponding to curve 5. Curve 3 corresponds to asymptotic bubble growth in the thermal regime of [3], defined by a constant overheating $\Delta T = T_0 - T_S(p_l)$. In this case $R \sim \sqrt{t}$. Curve 4 is an approximate analytical solution of the problem of bubble growth in a variable pressure field, obtained in [7]. This solution, obtained with the assumption that the thermal mechanism predominates and that the thermal boundary layer in the liquid is thin, generalizes the solution of [3] to the case of variable pressure. Certain differences between curves 1 and 4 are apparently related to the fact that in contrast to [7], the present study completely considers the effects of variation in the vapor properties. As is evident from Fig. 4, curves 1 and 4 describe the experiments satisfactorily, while the limiting curves 2 and 3 bracket the experimental points. We note that the data of [6] with decreasing pressure were obtained on preexisting bubbles. However, as was noted in [7], one cannot predict the type of thermal boundary layer existing in bubbles which have grown or collapsed, nor the effect of this layer on subsequent behavior.

Figure 5 shows computed radius–time curves for collapsing vapor bubbles in various liquids. Curves 1-5 show bubble behavior in water, Freon-12, nitrogen, hydrogen, and helium under identical initial conditions. The pressure in the liquids was instantaneously increased from $p_0 = 10^5$ Pa to $p_l = 12 \cdot 10^4$ Pa, with initial bubble radius $R_0 = 10$ μm, initial system temperature homogeneous and equal to the saturation temperature corresponding to equilibrium pressure in the bubble.

The behavior of curves 1-5 in Fig. 5 confirms the effectiveness of the parameter $B_0 = Ja^2 a_l / R_0 (\rho_l / \Delta p)^{1/2}$ introduced in [8] for predicting the character of vapor bubble collapse. Here $Ja = c_l \Delta T \rho_l / L \rho_{V0}$ is the Jacobi number, a_l is the thermal diffusivity of the liquid, $\Delta p = p_l - p_0$, $\Delta T = T_S(p_l) - T_0$. The parameter B_0 was defined in [8] as the ratio of the characteristic bubble collapse time $t_p = R_0 (\rho_l / \Delta p)^{1/2}$, if this process were limited only by liquid inertia, to the bubble combination time $t_T = R_0^2 / a_l Ja^2$, if the latter were determined solely by heat transfer. Thus, for large values of B_0 the bubble collapse process is close to the limiting inertial regime, while at low B_0 it is close to the thermal regime. Curves 1-5 in Fig. 5 correspond to values $B_0 = 8; 6 \cdot 10^{-2}; 10^{-2}; 5 \cdot 10^{-4}; 2 \cdot 10^{-4}$.

Figure 6 shows a comparison of calculated radius–time curves with experimental data [8] on collapse of air vapor bubbles in water under following initial conditions: $R_0 = 3.66$ mm, $p_0 = 636 \cdot 10^2$ Pa, $T_0 = T_S(p_0)$ (curve 1), $R_0 = 3.36$ mm, $p_0 = 734 \cdot 10^2$ Pa, $T_0 = T_S(p_0)$ (curve 2). In both cases the system was abruptly placed under an atmospheric pressure of $p_l = 10^5$ Pa, with the initial content of undissolved gas in the bubbles comprising $k = 0.0002, 0.0006$, respectively. To consider this fact curve 2 was also calculated with a system of equations for vapor-gas bubbles [9] (dashed line). Calculations showed that such a low gas content has practically no effect on the initial behavior of the radius–time curve, leading only to incomplete collapse of the bubbles.

For clarity the curves are shown with different scales: curve 1 corresponds to the left-hand vertical and upper horizontal axes, while curve 2 corresponds to the right-hand vertical and lower horizontal axes. The present results agree well with the experimental data. The dash–dot curve represents theoretical calculations of [10] for curve 1. In [10] an arbitrary assumption of parabolic velocity distribution of vapor particles in the bubble was used, leading to a distortion of the temperature profile. Moreover, as was noted in [1], the authors of [10] neglected the thermal flux into the vapor phase. However, as follows from the results of the present

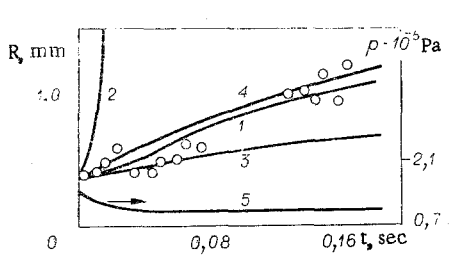

Fig. 4

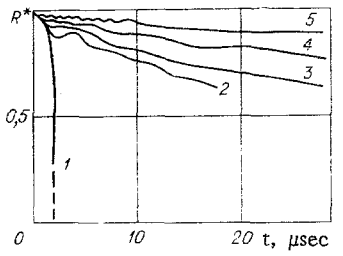

Fig. 5

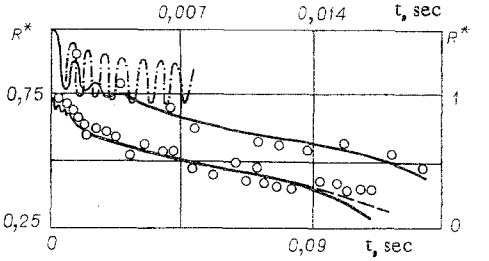

Fig. 6

study, the major shortcoming of [10], leading to significant divergence from experiment, was the improper choice of a step size in the finite difference system for the liquid energy equation. These steps should satisfy the condition $h_l \ll \delta_l$, where $\delta_l \sim (a_l/\omega)^{1/2}$ is the thickness of the temperature boundary layer in the liquid, $\omega = (3\gamma p_0/\rho_l)^{1/2}/R_0$ is the frequency of radial bubble oscillation. For the variant shown in Fig. 6, $\delta_l \sim 10^{-5}$ m, or $\delta_l \sim 0.3 \cdot 10^{-2} R_0$. Consequently, the step h_l should satisfy the condition $h_l \lesssim 10^{-3} R_0$. The choice in [10] of a coarser step ($h_l = 10^{-2} R_0$) led to a significant reduction in the liquid temperature gradient in the wall boundary layer, and thus to a significant reduction in phase transition rate, since, according to Eq. (2),

$$jl \approx \lambda_l \frac{\partial T_l}{\partial r}\Big|_R \leqslant \lambda_l \frac{\Delta T}{h_l},$$

whence

$$j/\rho_v \leqslant \frac{\lambda_l \Delta T}{h_l \rho_v}. \qquad (14)$$

Substituting in Eq. (14) the parameter values corresponding to the variant calculated in Fig. 6, with $h_l = 10^{-2} R_0$, we obtain $j/\rho_V \lesssim 0.2$ m/sec. At the same time $\dot{R} \sim (\Delta p/\rho_l)^{1/2} \approx 6$ m/sec. Consequently, with this choice of step $j/\rho_V \ll \dot{R}$, and according to Eq. (3) $w_V \approx \dot{R}$. The latter, if we also neglect the thermal flux into the vapor phase [10], leads by integration of Eq. (5) to the well-known relationship for an adiabatic gas bubble

$$p_v R^{3\gamma} = \text{const}.$$

Thus, the close agreement observed by the authors of [10] between their calculations and the behavior of a constant-mass adiabatic gas bubble, together with the divergence from the experimental results of [8] (no clear bubble pulsations observed), is hardly surprising.

The authors thank R. I. Nigmatulin for his interest in the study and for his valuable advice.

LITERATURE CITED

1. R. I. Nigmatulin and N. S. Khabeev, "Gas bubble dynamics," Izv. Akad. Nauk SSSR, Mekh. Zhidk. Gaza, No. 3 (1975).
2. R. I. Nigmatulin, Fundamentals of the Mechanics of Heterogeneous Materials [in Russian], Nauka, Moscow (1978).
3. M. S. Plesset and S. A. Zwick, "Growth of vapor bubbles in superheated liquids," J. Appl. Phys., 25, No. 4 (1954).
4. L. E. Scriven, "On the dynamics of phase growth," Chem. Eng. Sci., 10, No. 1 (1959).
5. L. D. Landau and E. M. Lifshits, Statistical Physics [in Russian], Nauka, Moscow (1964).
6. H. C. Hewitt and J. D. Parker, "Bubble growth and collapse in liquid nitrogen," Trans. ASME, J. Heat Trans., 90, No. 1 (1968).
7. O. C. Jones and N. Zuber, "Bubble growth in variable pressure fields," Trans. ASME, J. Heat Trans., 100, No. 3 (1978).
8. L. W. Florschuetz and B. T. Chao, "On the mechanics of vapor bubble collapse," Trans. ASME, J. Heat Trans., 87, No. 2 (1965).
9. R. I. Nigmatulin and N. S. Khabeev, "Gas bubble dynamics," Izv. Akad. Nauk SSSR, Mekh. Zhidk. Gaza, No. 6 (1976).
10. S. M. Cho and R. A. Seban, "On some aspects of steam bubble collapse," Trans. ASME, J. Heat Trans., 91, No. 4 (1969).